

Adsorption properties of OCN radical on (6,0), (8,0), and (10,0) zigzag single-walled carbon nanotubes: a density functional study

Mohammad T. Baei · S. Zahra Sayyed-Alangi ·
Alireza Soltani · Mahsa Bahari · Anis Masoodi

Received: 26 July 2010/Accepted: 31 October 2010/Published online: 26 November 2010
© Springer-Verlag 2010

Abstract The behavior of the OCN radical adsorbed on the external surface of H-capped (6,0), (8,0), and (10,0) zigzag single-walled carbon nanotubes was studied by using density functional calculations. Geometry optimizations were carried out at the B3LYP/6-31G* level of theory using the Gaussian 98 suite of programs. We present the nature of the OCN radical–surface interaction in selected sites of the nanotubes. Binding energies corresponding to adsorption of the OCN radical are calculated to be in the range 280–315 kJ mol⁻¹. More efficient binding energies cannot be achieved by increasing the nanotube diameter. We also provide the effects of OCN radical adsorption on the electronic properties of the nanotubes.

Keywords Nanotube · Adsorption · Binding energy · DFT

Introduction

Since the discovery of carbon nanotubes (CNTs) [1], single-walled carbon nanotubes (SWCNTs) have attracted great interest owing to their physical and chemical properties [1–3] and applications as a novel material [4, 5]. SWCNTs have a wide range of applications in nanoelectronics, nanoscaling biotechnology, and biosensors [3, 6–9]. Because of their size, large surface area, and hollow geometry,

SWCNTs are being considered as prime materials for gas adsorption [10–14]; biological, chemical, and electromechanical sensors; and nanoelectronic devices [15–17]. For example, CNTs have been experimentally investigated for the detection of gas molecules [18–20], organic vapors [21, 22], biomolecules, and different ions [23–25]. Doped or defective CNTs could give improved sensitivity when used in detecting molecules like CO, H₂O, 1,2-dichlorobenzene, or gaseous cyanide and formaldehyde [26–28]. The possibilities of using chemically doped CNTs as highly sensitive gas sensors are also under intensive investigation [18, 29]. Moreover, electronic conductance of a CNT semiconductor can be changed upon exposure to gas molecules, serving as a basis for nanotube molecular sensors.

Sensitivity of CNTs to the OCN radical has been indicated by means of quantum mechanics calculations. The determination of the structure of adsorbed cyanato radical (OCN) on CNT surfaces is also important for understanding its bonding and reactivity in catalysis and other surface phenomena. The OCN radical has been generated as an adsorbed product of the dissociative adsorption of hydrogen isocyanate (HNCO), and from the reaction of cyanogen (C₂N₂) and oxygen on Cu (100) [30], Cu (111) [31–33], and Cu (110) [34] surfaces. Moreover, adsorbed OCN was observed in the reaction of CO and NO over supported transition metal catalysts [35–37]. The understanding of the physisorption of the OCN radical on CNT surfaces is important for OCN storage. The objective of the present work was to study theoretically the interaction of the OCN radical with different adsorption sites on CNT surfaces and thereby to establish a deeper understanding of the physisorption of the OCN radical on different CNT surfaces. To our knowledge, a quantum mechanical study of the interaction of the OCN radical with CNT surfaces has not been reported.

M. T. Baei (✉) · S. Z. Sayyed-Alangi
Islamic Azad University, Azadshahr Branch,
Department of Chemistry, Azadshahr, Golestan, Iran
e-mail: Baei52@yahoo.com

A. Soltani · M. Bahari · A. Masoodi
Young Researchers Club, Islamic Azad University,
Gorgan Branch, Gorgan, Iran

Results and discussion

An OCN radical can approach the nanotube walls from outside (out), which is the most common case, and from the inside (in). Zigzag (6,0), (8,0), and (10,0) single-walled CNTs have two different C–C bonds (C1–C2 and C2–C3) (see Fig. 1; Table 1). For the adsorption of the OCN radical (N-down and O-down) on the CNTs, we considered four possible sites (i.e., the center site above the hexagon, and the C1, C2, and C3 sites above the carbon atoms) as described in Fig. 1. The notation N-down and O-down denotes an OCN perpendicular to the surface via N and O, respectively.

We limited our analysis to the interaction of OCN with the nanotubes' outer walls. Considering each site and

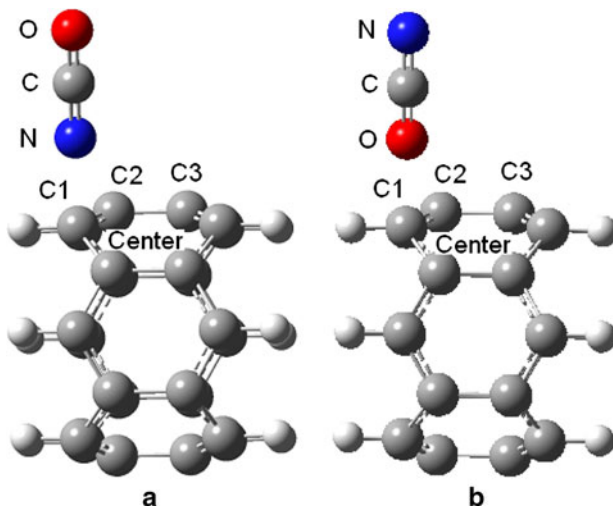


Fig. 1 Adsorption modes of an OCN radical on CNTs: N-down (left) and O-down (right)

configuration, we ended up with nine different approaches of OCN to the CNT walls. For each of these cases we investigated the CNT–OCN potential energy surface (PES). The binding energies of the OCN radical (N-down and O-down) at the four sites on zigzag (6,0), (8,0), and (10,0) single-walled CNTs are plotted in Fig. 2, and the binding energy with the equilibrium distance in each case is summarized in Table 1.

In all pathways the potential is attractive, presenting a well of maximum ca. -315 kJ mol^{-1} , which is characteristic of a chemisorption process. The binding energies obtained from these calculations are slightly dependent on orientations and locations of the OCN radical, and the interaction becomes rapidly repulsive as the molecule approaches the CNT wall. The calculated BE (binding energy) of the CNTs indicated that OCN may be absorbed on the sites with very small differences in total energy ($<13 \text{ kJ mol}^{-1}$) and the calculated BE for OCN in N-down is more than that in O-down. The most stable configuration of OCN for N-down in the (6,0) CNT is the C1 site, the perpendicular approach of OCN (N-down) radical to the (6,0) CNT wall on the upper carbon atom, and the current calculation shows that the adsorption energy for this site is $-293.74 \text{ kJ mol}^{-1}$ with equilibrium distance (rd) 2 Å. The most stable configurations of OCN for N-down in the (8,0) and (10,0) CNTs are the C2 and center site, respectively. The current calculation showed that the adsorption energies for these sites are -298.75 and $-308.11 \text{ kJ mol}^{-1}$ with equilibrium distance (rd) 3.0 and 2.0 Å, respectively. We observed that when the CNT diameter increases, the binding energy of OCN also increases at each particular site of the interaction by very little ($<13 \text{ kJ mol}^{-1}$). For example, OCN (N-down) binds on the site C1 of a (6,0) CNT with $-293.74 \text{ kJ mol}^{-1}$, whereas it binds on the C2 site of a (8,0)

Table 1 Binding energy value (kJ mol^{-1}), equilibrium distance (Å) (rd), and energy gap (eV) of an OCN radical on zigzag (6,0), (8,0), and (10,0) CNTs

Model	$R_{\text{C-C}}$ (Å)	Mode	Site				
			C1	C2	C3	Center	
(6,0)	$\text{C1-C2} = 1.418$	N-down	Binding energy	-293.74	-286.65	-280.93	-293.01
		rd		2.0	3.0	3.0	3.0
	$\text{C2-C3} = 1.452$	O-down	Binding energy	-282.46	-283.45	-277.28	-286.29
		rd		3.5	3.0	3.0	3.0
(8,0)	$\text{C1-C2} = 1.411$	N-down	Binding energy	-295.24	-298.75	-292.71	-293.73
		rd		3.0	3.0	3.0	3.0
	$\text{C2-C3} = 1.460$	O-down	Binding energy	-283.84	-288.01	-290.33	-294.55
		rd		3.5	3.0	3.0	3.0
(10,0)	$\text{C1-C2} = 1.408$	N-down	Binding energy	-303.79	-298.88	-298.84	-308.11
		rd		2.5	2.0	2.0	2.0
	$\text{C2-C3} = 1.464$	O-down	Binding energy	-285.14	-294.47	-295.51	-301.56
		rd		3.0	2.5	2.0	2.0

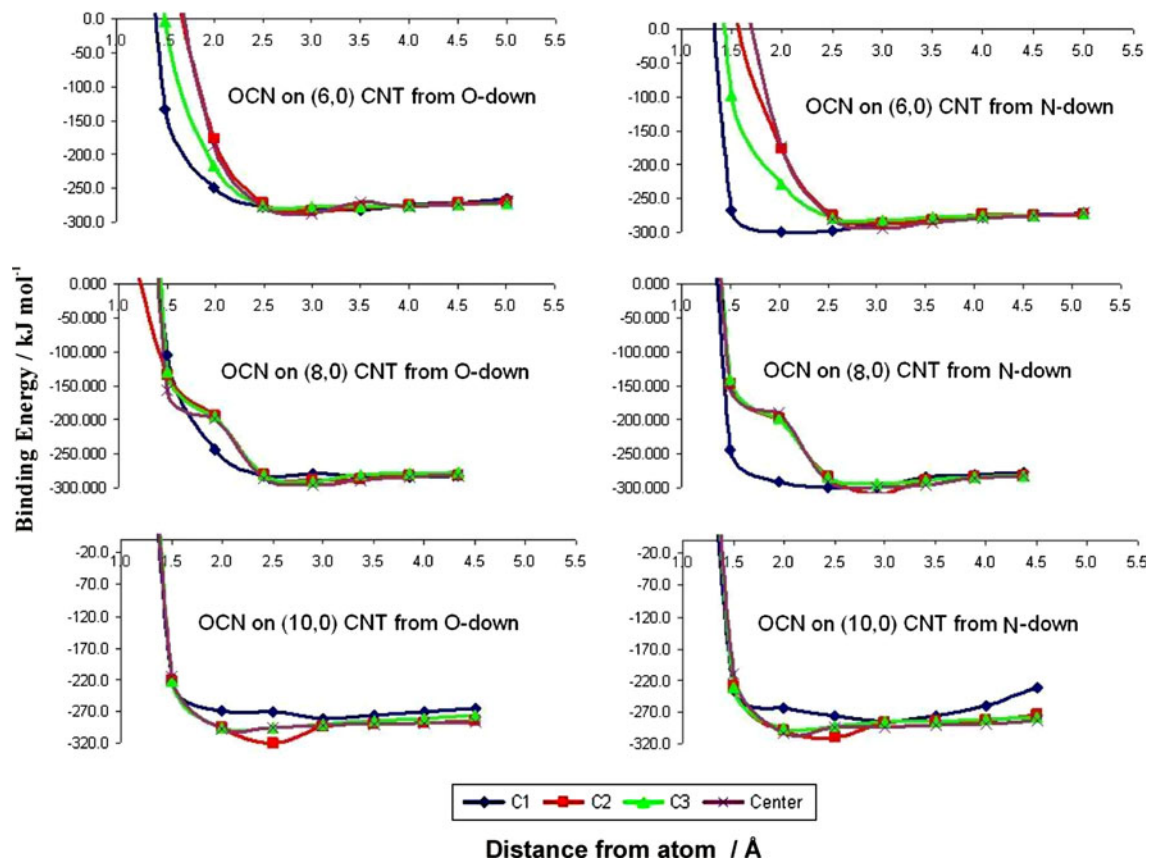


Fig. 2 Binding energy curves of OCN radical (O-down and N-down) adsorption at C1, C2, C3, and center sites on zigzag (6,0), (8,0), and (10,0) CNTs

CNT with $-298.75 \text{ kJ mol}^{-1}$ or on the center site of a (10,0) CNT with $-308.11 \text{ kJ mol}^{-1}$. Therefore, the binding energy of the OCN radical from (6,0) to (8,0) and from (8,0) to (10,0) CNTs increases by 1.67 and 3.04%, respectively. An interesting conclusion that can be drawn from these pathways is that only the type of the tube (CNT) plays an important role in determining the binding energy of the OCN radical and not the diameter of the tube as observed in previous cases. All results are clearly demonstrated in Table 1.

Electronic properties

Finally, we studied the influence of OCN radical adsorptions on the electronic properties of the CNTs. The calculated band gaps of the clean perfect (6,0), (8,0), and (10,0) single-walled CNTs are about 0.59, 0.73, and 0.89 eV, respectively, and these values are very close those derived from density functional theory (DFT) simulations for other small diameter zigzag tubes [38, 39]. The effects of the OCN radical on adsorption energies in the CNTs relate to their electronic structure. When the OCN radical is adsorbed on the CNTs, the interaction between them being strong, the electronic properties of these tubes are changed

obviously. It is clear that the presence of the OCN radical increases the energy gap of pristine CNTs. With the OCN radical adsorption, the band gaps are calculated to be about 1.15, 0.91, and 1.06 eV for (6,0), (8,0), and (10,0) single-walled CNTs, respectively. However, the adsorption of the OCN radical further increases the band gap. In this study, the presence of the OCN radical slightly increases the energy gap of pristine CNTs, and reduces their electrical conductance.

In summary, we theoretically studied the adsorptions of the OCN radical on zigzag (6,0), (8,0), and (10,0) single-walled CNTs through DFT calculations. On the basis of our calculations, it seems that pristine CNTs can be used as an OCN storage medium as long as OCN is adsorbed on the exterior walls of the CNTs because of the high binding energy. Comparing all the binding energy curves of the OCN radical interacting with all possible sites of adsorption on nanotube walls and in several structural configurations, one can easily conclude the more efficient binding modes of the OCN radical. For the CNTs the calculated BE for OCN in N-down is a little more than that in O-down. We showed that by increasing the nanotube diameter more efficient binding could not be achieved. Furthermore, in this study the

presence of the OCN radical slightly increases the energy gap of pristine CNTs and reduces their electrical conductance.

Methods

In the present work, adsorption behaviors of the OCN radical on SWCNTs were studied by using the representative models of (6,0), (8,0), and (10,0) zigzag single-walled CNTs in which the ends of nanotubes are saturated by hydrogen atoms. The hydrogenated (6,0), (8,0), and (10,0) zigzag single-walled CNTs have 36 ($C_{24}H_{12}$), 48 ($C_{32}H_{16}$), and 60 ($C_{40}H_{20}$) atoms, respectively. In the first step, the structures were allowed to relax by all atomic geometrical optimization at the DFT level of B3LYP exchange-functional and 6-31G* standard basis set. The optimized structures have diameters of ~ 4.80 , 6.33 , and 7.88 \AA , respectively. The binding energy of an OCN radical on the CNT wall was calculated as follows:

$$\text{BE} = E_{\text{CNT-OCN}} - (E_{\text{CNT}} + E_{\text{OCN}}) \quad (1)$$

where $E_{\text{CNT-OCN}}$ was obtained from the scan of the potential energy of the CNT molecular cyanato structure, E_{CNT} is the energy of the optimized CNT structure, and E_{OCN} is the energy of an optimized OCN radical. All the calculations were carried out by using the Gaussian 98 suite of programs [40].

Acknowledgments This work was financially supported by Islamic Azad University, Azadshahr Branch.

References

- Iijima S (1991) *Nature* 354:56
- Derycke V, Martel R, Appenzeller J, Avouris P (2002) *Appl Phys Lett* 80:2773
- Liu C, Fan YY, Liu M, Cong HT, Cheng HM, Dresselhaus MS (1999) *Science* 286:1127
- Zurek B, Autschbach J (2004) *J Am Chem Soc* 126:13079
- Nojeh A, Lakatos GW, Peng S, Cho K, Pease RFW (2003) *Nano Lett* 3:1187
- Zhou O, Shimoda H, Gao B, Oh SJ, Fleming L, Yue G (2002) *Acc Chem Res* 35:1045
- Zhen Y, Postma HWC, Balents L, Dekker C (1999) *Nature* 402:273
- Baughman RH, Cui C, Zakhidov AA, Iqbal Z, Barisci JN, Spinks GM, Wallace GG, Mazzoldi A, Rossi DD, Rinzler AG, Jaschinski O, Roth S, Kertesz M (1999) *Science* 284:1340
- Gao H, Kong Y, Cui D, Ozkan CS (2003) *Nano Lett* 3:471
- Rawat DS, Calbi MM, Migone AD (2007) *J Phys Chem C* 111:12980
- Zhao J, Buldum A, Han J, Lu JP (2002) *Nanotechnology* 13:195
- Gordillo MC (2007) *Phys Rev B* 76:115402
- Choi YS, Park KA, Kim C, Lee YH (2004) *J Am Chem Soc* 126:9433
- Byl O, Kondratyuk P, Forth ST, Fitzgerald SA, Chen L, Johnson JK, Yates Jr JT (2003) *J Am Chem Soc* 125:5889
- Yang X, Lu Y, Ma Y, Liu Z, Du F, Chen Y (2007) *Biotech Lett* 29:1775
- Gowtham S, Scheicher RH, Ahuja R, Pandey R, Karna S (2007) *Phys Rev B* 75:033401
- Froudakis GE, Schnell M, Muhlhaeser M, Peyerimhoff SD, Andriots AN, Menon M, Sheetz RM (2003) *Phys Rev B* 68:115435
- Kong J, Franklin NR, Zhou C, Chapline MG, Peng S, Cho K, Dai H (2000) *Science* 287:622
- Bekyarova E, Davis M, Burch T, Itkis ME, Zhao B, Sunshine S, Haddon RC (2004) *J Phys Chem B* 108:19717
- Feng X, Irle S, Witek H, Morokuma K, Vidic R, Borguet E (2005) *J Am Chem Soc* 127:10533
- Li J, Lu Y, Ye Q, Cinke M, Han J, Meyyappan M (2003) *Nano Lett* 3:929
- Agnihotri S, Mota JPB, Rostam-Abadi M, Rood MJ (2006) *J Phys Chem B* 110:7640
- Chen RJ, Choi HC, Bangsaruntip S, Yenilmez E, Tang X, Wang Q, Chang YL, Dai H (2004) *J Am Chem Soc* 126:1563
- Chen RJ, Zhang Y, Wang D, Dai H (2001) *J Am Chem Soc* 123:3838
- Kam NWS, Dai H (2005) *J Am Chem Soc* 127:6021
- Peng S, Cho K (2003) *Nano Lett* 3:513
- Fagan SB, Filho AGS, Lima JOG, Filho JM, Ferreira OP, Mazali IO, Alves OL, Dresselhaus MS (2004) *Nano Lett* 4:1285
- Zhang Y, Zhang D, Liu C (2006) *J Phys Chem B* 110:4671
- Collins PG, Bradley K, Ishigami M, Zettl A (2000) *Science* 287:1801
- Celio H, Mudalige K, Mills P, Trenary M (1997) *Surf Sci* 394:L168
- Solymosi F, Kiss J (1981) *Surf Sci* 104:181
- Solymosi F, Kiss J (1981) *Surf Sci* 108:368
- Kordes ME, Stenzel W, Conrad H, Weaver MJ (1987) *J Am Chem Soc* 109:1878
- Oukta DA, Jorgensen SW, Friend CM, Madix RJ (1983) *J Mol Catal* 21:375
- Kostov KL, Jakob P, Rauscher H, Menzel D (1991) *J Phys Chem* 95:7785
- Jakob P (1996) *Chem Phys Lett* 263:607
- Guo X, Winkler A, Chorkendorff I, Hagans PL, Siddiqui HR, Yates JT Jr (1988) *Surf Sci* 203:17
- Yim WL, Liu ZF (2004) *Chem Phys Lett* 398:297
- Zhang YF, Liu ZF (2004) *J Phys Chem B* 108:11435
- Frisch MJ, Trucks GW, Schlegel HB, Scuseria GE, Robb MA, Cheeseman JR, Zakrzewski VG, Montgomery JA Jr, Stratmann RE, Burant JC, Dapprich S, Millam JM, Daniels AD, Kudin KN, Strain MC, Farkas O, Tomasi J, Barone V, Cossi M, Cammi R, Mennucci B, Pomelli C, Adamo C, Clifford S, Ochterski J, Petersson GA, Ayala PY, Cui Q, Morokuma K, Malick DK, Rabuck AD, Raghavachari K, Foresman JB, Cioslowski J, Ortiz JV, Baboul AG, Stefanov BB, Liu G, Liashenko A, Piskorz P, Komaromi I, Gomperts R, Martin RL, Fox DJ, Keith T, Al-Laham MA, Peng CY, Nanayakkara A, Gonzalez C, Challacombe M, Gill PMW, Johnson B, Chen W, Wong MW, Andres JL, Gonzalez C, Head-Gordon M, Replogle ES, Pople JA (1998) Gaussian 98. Gaussian, PA